Universal Photonic Quantum Interface for a Quantum Network

Jian Wang,[1,2] Yun-Feng Huang,[1,2,*] Chao Zhang,[1,2] Jin-Ming Cui,[1,2] Zhi-Yuan Zhou,[1,2] Bi-Heng Liu,[1,2] Zong-Quan Zhou,[1,2] Jian-Shun Tang,[1,2] Chuan-Feng Li,[1,2,†] and Guang-Can Guo[1,2]

[1]*CAS Key Laboratory of Quantum Information, University of Science and Technology of China, Hefei 230026, P.R. China*

[2]*CAS Center For Excellence in Quantum Information and Quantum Physics, University of Science and Technology of China, Hefei 230026, P.R. China*

Active research on mesoscopic quantum systems has increased our understanding of and ability to control quantum objects, allowing the construction of a universal form for quantum networks that consist of more than one physical system. This kind of quantum network is anticipated to enable the building of quantum infrastructure, such as long-distance quantum communication and distributed quantum computers, and motivates the establishment of photonic quantum interfaces that are compatible with physical systems. Here, a universal photonic quantum interface is experimentally developed with the benefit of a unique, specially designed entangled photon source. The detailed experimental results show that this configuration can satisfy all the urgent demands for a photonic quantum interface, including the accurate matching of the working wavelength and bandwidth and specifically, the entanglement ability ($F = 89.6\%$, $S = 2.36 \pm 0.03$). The realization of this universal photonic quantum interface is expected to expedite the construction of much more complex quantum networks and to be a major step in the area of optical engineering and control.

I. INTRODUCTION

The high-level manipulation of single quantum systems provides opportunities to research much larger and more complex quantum systems, which is considered essential to implement quantum networks [1–3]. A quantum network has been proved to be a promising method for long-distance quantum communication and large-scale distributed quantum computing. Compared with the rapid development of a quantum network consisting of identical physical systems [4–8], relatively little work, in recent years, has focused on the universal form of a quantum network consisting of various physical systems [9–12]. The advantages of this kind of quantum network are that it can unite the benefits and avoid the inherent limitations of the different physical systems, offering the possibility of constructing higher-performance quantum systems [13–16]. However, this development process also leads to an urgent demand for universal photonic quantum interfaces that are compatible with the various physical systems [17]. In particular, the large working frequency mismatching of physical systems and the requirements of some nonclassical correlations between them bring urgent outstanding challenges to building a universal quantum network.

To serve as a universal photonic quantum interface, a system should simultaneously satisfy three key elements. With respect to the first two elements, the central frequencies and bandwidths of the photons should perfectly match those of the stationary physical systems, thus ensuring the maximum possibility of interaction between the traveling photons and the stationary physical systems. With respect to the third element, the framework should have the ability to entangle stationary physical systems into a larger quantum system, which has been proved to be the key resource of quantum-information processing tasks. Some experimental progress has been achieved to show that the working frequency mismatching of central frequencies can be compensated with methods such as coherent frequency conversion [17,18], tailoring one frequency to be compatible with another one [9,10] or the generation of a narrow-band photon source [19,20]. The bandwidths of photons have also been tailored with spectral shaping techniques [21,22]. Because the fragility of entanglement causes it to be affected by the environment, studies on the generation of the appearance of entanglement in a process are rare, and entanglement is also the most challenging element in the generation of universal quantum interfaces. Even though many efforts have addressed different aspects of the above three elements, a universal quantum interface simultaneously satisfying all the key elements has not been realized to date.

*hyf@ustc.edu.cn
†cfli@ustc.edu.cn

Here, we report the first generation of this kind of universal quantum interface via a cavity-enhanced nondegenerate narrow-band-entangled photon source, which can perfectly satisfy the aforementioned urgent needs. In the area of cavity-enhanced photon sources, nonlinear processes occur in a nonlinear material that is surrounded by an optical cavity, and the generated photons that are matched with the cavity mode are greatly enhanced in brightness with a narrow bandwidth depending on the cavity design [23–27]. Many such types of photon sources have been experimentally achieved [27–31], promoting the developments of quantum networks and quantum metrology [32–34]. In this work, to realize a universal quantum interface, the nondegenerate narrow-band-entangled photon source consists of a customized conjoined double-cavity structure. Due to the merits of this type of cavity structure, the double cavities can be precisely locked independently to two different reference frequencies, and the bandwidth matching can be realized by modifying the inherent properties of the optical cavities. Most importantly, this design of the cavity structure allows the entangling of different stationary physical systems.

Specifically, the central frequencies and bandwidths of this photon source are compatible with those of trapped ions and rare earth-doped solid-state quantum-memory systems. Trapped ions have been verified as an advanced physical system for quantum computation and quantum simulations [35,36], and rare earth-doped crystals have shown reliable performance and a high storage capacity for quantum memory [10,37]. With a compatible photonic interface, this capability enables the construction of the perfect quantum network described by Kimble [1]. The entanglement here is directly generated at the output of the cavity and is verified by quantum-state tomography (fidelity = 89.6%) and a Bell-type inequality violation ($S = 2.36 \pm 0.03$).

II. EXPERIMENTAL FRAMEWORK

The experimental scheme of our photon-pair source, shown in Fig. 1, consists mainly of two parts: the 453-nm pump laser generation part and the cavity-enhanced spontaneous parametric downconversion (SPDC) process. The pump laser is generated through the sum-frequency generation (SFG) process with a periodically poled KTiOPO4 (PPKTP) in a bowtie cavity [38]. The 935-nm laser (Toptica) and 880-nm laser (Ti sapphire) provide the power to generate the 453-nm pump laser and to lock the optical cavities in the SPDC part. It is essential to obtain the pump laser using the SFG process in this kind of experiment, and the SFG process in the bowtie cavity structure provides a highly efficient pump laser with a pure optical mode. In the cavity-enhanced SPDC process part, two identically fabricated type-II PPKTPs are used to generate the photon pairs. The calculated theoretical bandwidth of

the phase matching in the PPKTPs is 120 GHz. To obtain the polarization-entangled photon pairs, we place the two PPKTPs side-by-side with their optical axes perpendicular to each other, and the polarization of the pump laser is oriented with an angle of 45° relative to the horizontal direction [39]. In this case, the generated polarization-entangled state is

$$|\psi\rangle = \frac{1}{\sqrt{2}}(|H_i\rangle|V_s\rangle + |V_i\rangle|H_s\rangle), \qquad (1)$$

where s and i represent the 935-nm signal photon and the 880-nm idler photon, respectively.

For a cavity-enhanced SPDC process, the modes of all the generated photons should match with the cavity modes. According to Eq. (1), four different modes of photons should match the cavity modes simultaneously, which is impossible to realize in a single cavity [40]. To solve this issue, a specially designed conjoined double-cavity (CDC) structure is used in conjunction with a customized dichroic mirror (DM) in it, as the dotted box shows in Fig. 1. With the DM, the 935-nm and 880-nm downconverted photons are divided into two cavities and are independently matched with their corresponding cavity; thus, in one cavity, only two cavity modes, corresponding to a single frequency, need to match, which makes the experiment feasible. The optical birefringent wedges are used here to compensate the nondegeneration of the polarization modes, which is simple, more compact, and more efficient than previous methods [30]. In particular, this approach decreases the urgent demand of the overall temperature-controlling accuracy (less than 1 mK) of the system. Since the phase deviation of the entangled state is greatly enhanced by the cyclical effect of the optical cavity, where the phase deviation mainly originates from tiny changes of the overall temperature and small vibrations of the system, precise temperature control of the nonlinear crystals and careful vibration isolation are experimentally pursued to ensure that the phase of the entangled state is stabilized in this process. Additionally, in the experiment, five birefringent components are inserted into the cavity to generate the entanglement, including one DM, two nonlinear crystals, and two optical wedges. Due to the enhanced cyclical effect of the optical cavity, any small misalignments of the optical axes of these birefringent components will cause rotations of the polarization modes in the optical cavity, which works as a compound of waveplates [41]. This condition will cause the mixing of the output photons' polarization modes, which decreases the fidelity of the entangled state. To address this problem, the birefringent components are mounted flexibly and aligned precisely one-by-one to suppress these effects. More details about the SFG progress and cavity-SPDC process are described in the Supplemental Material [42].

The cavities are locked to the reference laser beams using the Pound-Drever-Hall method [43]. The mechanical
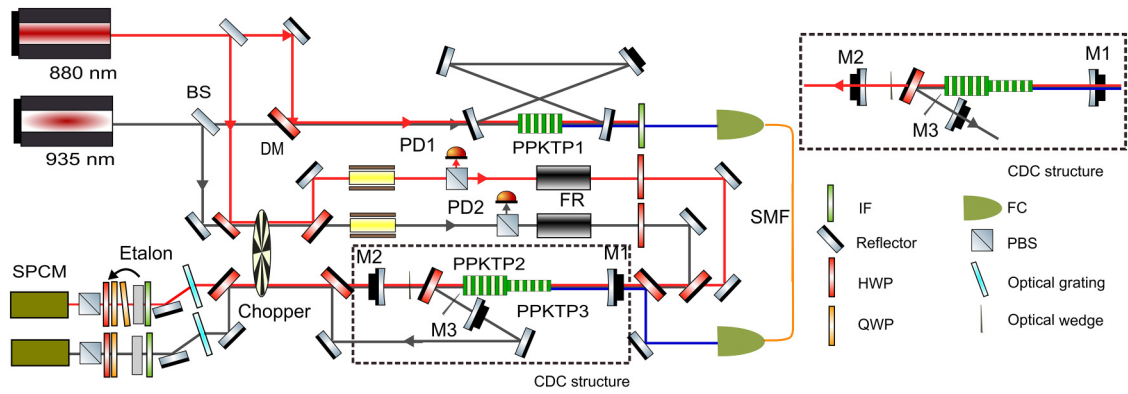
FIG. 1. Experimental configuration. BS, beam splitter; DM, dichroic mirror; IF, interference filter; FC, fiber coupler; HWP, half-wave plate; QWP, quarter-wave plate; PBS, polarization beam splitter; EOM, electro-optic modulator; FR, Faraday rotator; PD1, PD2, photodiodes; SMF, single-mode fiber; SPCM, single-photon counting module. The red line here represents the 880-nm laser and photon, the grey line represents the 935-nm laser and photons, and the blue line represents the 453-nm pump laser. The subfigure is the CDC structure. The core device is a DM that can separate two different photons into two optical cavities. The two optical cavities are conjoined by the shared input cavity mirror, nonlinear crystals, and the DM.

chopper is used as before to intermittently lock the cavities to protect the single-photon detector. In the nondegenerate case, due to the inevitable difference frequency generation (DFG) processes in the cavity, the best method to lock the cavity is to use only one chopper. Two locking beams and SPDC photon pairs are combined, and pass through the chopper together, which will ensure that a strong laser beam cannot leak through the chopper to damage the single-photon detectors. Two temperature-controlled (10 mK) optical etalons (central wavelengths 935 and 880 nm, bandwidth 120 MHz, free spectral range 8.4 GHz) are used to filter out the extra multimode components in the cavity outputs.

III. RESULTS

To verify the entanglement property of the photon source, we first measure the polarization correlations with adjustable polarization analyzers, each consisting of an HWP, a QWP, and a PBS. The analyzer of the 880-nm wavelength is set to $-45°$, while the analyzer of the 935-nm wavelength is varied by rotating its HWP. The results are shown in Fig. 2. We also conduct the Clauster-Horne-Shimony-Holt (CHSH) inequality test and obtain $S = 2.36 \pm 0.03$, which means that the violation is 12 standard deviations. To obtain the full characterization of the generated entangled photon source, we also perform quantum-state tomography and reconstruct the density matrix, which is shown in Fig. 3. From the tomography result, we obtain a state fidelity of 89.6% between the generated state and the targeted Bell state $|\psi\rangle$.

The bandwidth of the photon source is inversely proportional to the correlation time between the generated signal and the idler photons. Therefore, we conduct the time-correlated measurements, specifically to measure the

second-order cross-correlation function, $G_{S,I}^{(2)}(\tau)$, between the signal and the idler photons. The time distribution of photon pairs arriving at the detectors is recorded by the time-to-digital converter (Picoquant 400). The measured result is plotted in Fig. 4. We use the fitting function $e^{-2\pi\Delta\upsilon\tau}$ to fit the two sides of the curve separately and obtain the signal and the idler photon bandwidths are 9 MHz at 935 nm and 9.5 MHz at 880 nm. The small difference is the source of the different losses of the inserted optical devices at the two wavelengths.

Due to the properties of the optical cavity, the generated cavity-enhanced narrow-band photon pair often has a comblike multimode structure in the frequency domain,
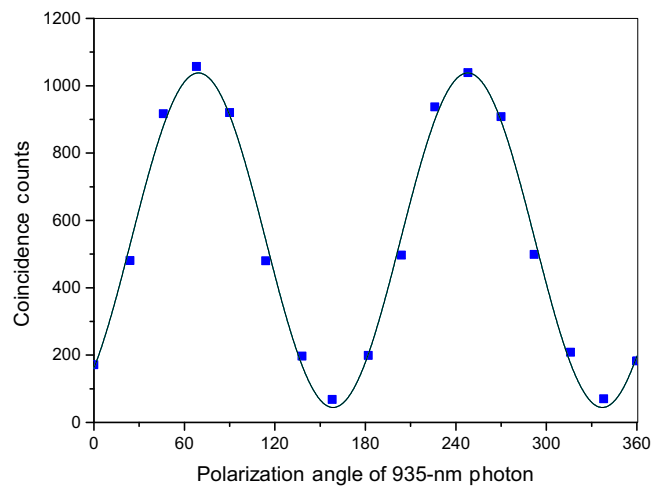

FIG. 2. Polarization correlation for the entangled photon source. The coincidence time window here is 80 ns. The pump power is 9 mW and the integration time is 200 s. The angle from the horizontal axis is measured in degrees.
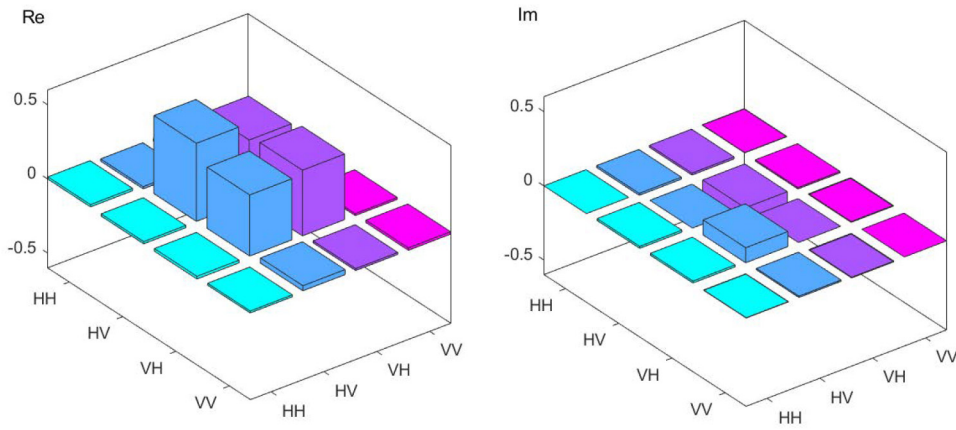
FIG. 3. Entangled state tomography results. Left, real part; right, imaginary part.

which strongly degrades the coherence of the source. In our experiment, we insert two FP etalons into the two outports of the photon source to filter the additional multi-mode components. To compare the unfiltered and filtered cases, we take the time-resolved measurement of the cross-correlated function $G_{S,I}^{(2)}(\tau)$ on the output photon pairs in both cases. For the existence of multimode photons, the time-resolved measurement of $G_{S,I}^{(2)}(\tau)$ produces a time-domain comblike structure of the curve, resulting from the interference between different frequency modes. In contrast, the time-domain comblike structure disappears under efficient elimination of multimode components. The results are shown in Fig. 5. The relatively smooth curve indicates that the multimode components in the source are efficiently filtered.

The rate of the single-mode photon-pair source is approximately 5 s at a pump power of 9 mW. Therefore, the normalized spectrum brightness is approximately 0.062/s/MHz/mW without any modification, and has a fidelity of 89.6% between the generated quantum state with a Bell state. However, these values have significant potential to improve by this method. The low counting rate is

caused mainly by the intracavity loss and the low detector efficiencies. For the fidelity of the photon-pair source, as an advantage of the source, no postselection gives a strong demand on the stabilization of phase in the entangled state and precise alignment of the optical axis of the five inserted birefringent devices. Additionally, we detect strong noise in the PPKTP crystals, which decreases the signal-to-noise ratio and limits the 453-nm pump power. All these factors can be improved by using much better equipment. More details can be obtained in the Supplemental Material [42].

IV. DISCUSSION

In addition to the method realized in this manuscript, other research efforts exist to realize the photonic quantum interface, mainly including tailoring one frequency to be compatible with another or using coherent frequency conversion [17,18]. It is straightforward to propose the method of tailoring one frequency to be compatible with another
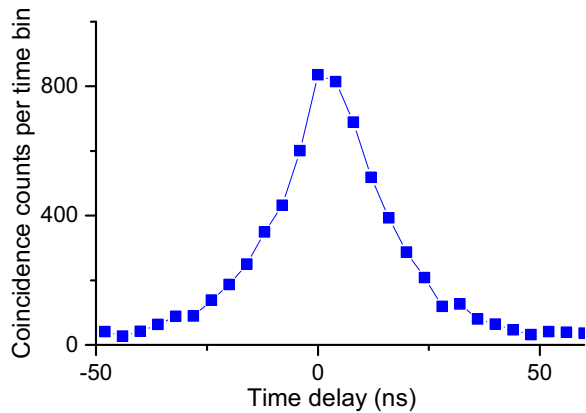

FIG. 4. Correlation function $G_{S,I}^{(2)}(\tau)$ measured at a pump power of 9 mW. The time-bin size is 4 ns and the integration time is 1800 s.
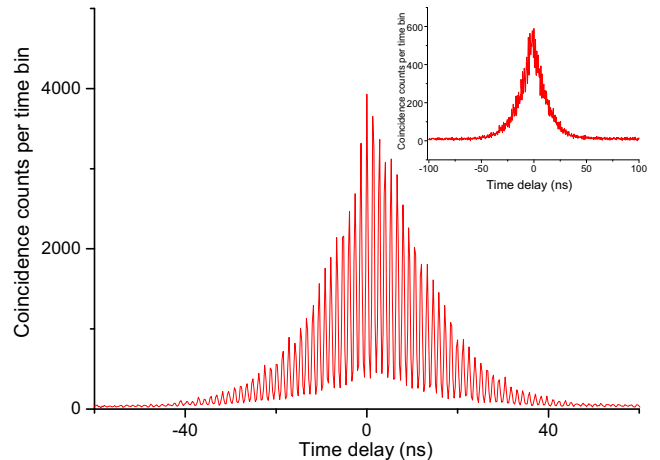

FIG. 5. Time-resolved measurement of correlation function $G_{S,I}^{(2)}(\tau)$ is performed at a pump power of 9 mW. The time-bin size is 256 ps, and the integration time is 600 s. The inset is measured with etalons used to filter the multimode components. The pump power is also 9 mW and the integration time is 3600 s.

[9,10], and this strategy is the same for interfacing two identical physical systems, such as a trapped ion system [44] or a single cold neutral atom system [4]. However, in fact, there are only a few kinds of physical systems, such as quantum dots for which the working wavelength can be tailored. Therefore, this method can not be a universal photonic quantum interface. Coherent frequency conversion is another method to realize a photonic quantum interface. This method generates problems if the physical system cannot emit the photons, such as the quantum memory used in this manuscript. Additionally, in the above two methods, a common limitation is that the bandwidth is very difficult to change to match various physical systems. For entanglement, no works to date have reported the tailoring frequency method. In contrast to the two aforementioned methods, the method described here can provide a universal photonic quantum interface based on the results of this work.

V. CONCLUSIONS

In conclusion, we realize a universal photonic quantum interface for a quantum network using a nondegenerate narrow-band-entangled photon source. This approach satisfies the needs for a photonic interface because it can match the central frequencies and bandwidths of different kinds of quantum nodes perfectly and has the ability to entangle these components into a larger network. The realization of this universal photonic quantum interface will hasten the construction of a quantum network and enrich the ability to engineer it using photons.

ACKNOWLEDGMENTS

[1] H. J. Kimble, The quantum internet, Nature **453**, 1023 (2008).

[2] L.-M. Duan and C. Monroe, Colloquium: Quantum networks with trapped ions, Rev. Mod. Phys. **82**, 1209 (2010).

[3] I. A. Walmsley and J. Nunn, Editorial: Building Quantum Networks, Phys. Rev. Appl. **6**, 040001 (2016).

[4] S. Ritter, C. Nölleke, C. Hahn, A. Reiserer, A. Neuzner, M. Uphoff, M. Mücke, E. Figueroa, J. Bochmann, and G. Rempe, An elementary quantum network of single atoms in optical cavities, Nature **484**, 195 (2012).

[5] H. Bernien, B. Hensen, W. Pfaff, G. Koolstra, M. S. Blok, L. Robledo, T. H. Taminiau, M. Markham, D. J. Twitchen, L. Childress, and R. Hanson, Heralded entanglement between solid-state qubits separated by three metres, Nature **497**, 86 (2013).

[6] I. Usmani, C. Clausen, F. Bussières, N. Sangouard, M. Afzelius, and N. Gisin, Heralded quantum entanglement between two crystals, Nat. Photonics **6**, 234 (2012).

[7] Z.-S. Yuan, Y.-A. Chen, B. Zhao, S. Chen, J. Schmiedmayer, and J.-W. Pan, Experimental demonstration of a BDCZ quantum repeater node, Nature **454**, 1098 (2008).

[8] D. Hucul, I. Inlek, G. Vittorini, C. Crocker, S. Debnath, S. Clark, and C. Monroe, Modular entanglement of atomic qubits using photons and phonons, Nat. Phys. **11**, 37 (2015).

[9] H. Meyer, R. Stockill, M. Steiner, C. Le Gall, C. Matthiesen, E. Clarke, A. Ludwig, J. Reichel, M. Atatüre, and M. Köhl, Direct Photonic Coupling of a Semiconductor Quantum Dot and a Trapped Ion, Phys. Rev. Lett. **114**, 12 (2015).

[10] J.-S. Tang, Z.-Q. Zhou, Y.-T. Wang, Y.-L. Li, X. Liu, Y.-L. Hua, Y. Zou, S. Wang, D.-Y. He, G. Chen, Y.-N. Sun, Y. Yu, M.-F. Li, G.-W. Zha, H.-Q. Ni, Z.-C. Niu, C.-F. Li, and G.-C. Guo, Storage of multiple single-photon pulses emitted from a quantum dot in a solid-state quantum memory, Nat. Commun. **6**, 8652 (2015).

[11] R. W. Andrews, R. W. Peterson, T. P. Purdy, K. Ci-cak, R. W. Simmonds, C. A. Regal, and K. W. Lehnert, Bidirectional and efficient conversion between microwave and optical light, Nat. Phys. **10**, 321 (2014).

[12] N. Maring, P. Farrera, K. Kutluer, M. Mazzera, G. Heinze, and H. de Riedmatten, Photonic quantum state transfer between a cold atomic gas and a crystal, Nature **551**, 485 (2017).

[13] M. Wallquist, K. Hammerer, P. Rabl, M. Lukin, and P. Zoller, Hybrid quantum devices and quantum engineering, Phys. Scr. **T137**, 014001 (2009).

[14] Z.-L. Xiang, S. Ashhab, J. You, and F. Nori, Hybrid quantum circuits: Superconducting circuits interacting with other quantum systems, Rev. Mod. Phys. **85**, 623 (2013).

[15] G. Kurizki, P. Bertet, Y. Kubo, K. Mølmer, D. Petrosyan, P. Rabl, and J. Schmiedmayer, Quantum technologies with hybrid systems, PNAS **112**, 3866 (2015).

[16] S. Kotler, R. W. Simmonds, D. Leibfried, and D. J. Wineland, Hybrid quantum systems with trapped charged particles, Phys. Rev. A **95**, 022327 (2017).

[17] S. Tanzilli, W. Tittel, M. Halder, O. Alibart, P. Baldi, N. Gisin, and H. Zbinden, A photonic quantum information interface, Nature **437**, 116 (2005).

[18] S. Ramelow, A. Fedrizzi, A. Poppe, N. K. Langford, and A. Zeilinger, Polarization-entanglement-conserving frequency conversion of photons, Phys. Rev. A **85**, 013845 (2012).

[19] T.-M. Zhao, H. Zhang, J. Yang, Z.-R. Sang, X. Jiang, X.-H. Bao, and J.-W. Pan, Entangling Different-Color Photons via Time-Resolved Measurement and Active Feed Forward, Phys. Rev. Lett. **112**, 103602 (2014).

[20] J. Wang, P.-Y. Lv, J.-M. Cui, B.-H. Liu, J.-S. Tang, Y.-F. Huang, C.-F. Li, and G.-C. Guo, Generation of Nondegenerate Narrow-Band Photon Pairs for a Hybrid Quantum Network, Phys. Rev. Appl. **4**, 064011 (2015).

[21] K. A. Fisher, D. G. England, J.-P. W. MacLean, P. J. Bustard, K. J. Resch, and B. J. Sussman, Frequency and bandwidth conversion of single photons in a room-temperature diamond quantum memory, Nat. Commun. **7**, 11200 (2016).

[22] J. Lavoie, J. M. Donohue, L. G. Wright, A. Fedrizzi, and K. J. Resch, Spectral compression of single photons, Nat. Photonics **7**, 363 (2013).

[23] K.-H. Luo, H. Herrmann, S. Krapick, B. Brecht, R. Ricken, V. Quiring, H. Suche, W. Sohler, and C. Silberhorn, Direct generation of genuine single-longitudinal-mode narrowband photon pairs, New J. Phys. **17**, 073039 (2015).

[24] C. Reimer, M. Kues, L. Caspani, B. Wetzel, P. Roztocki, M. Clerici, Y. Jestin, M. Ferrera, M. Peccianti, A. Pasquazi, B. E. Little, S. T. Chu, D. J. Moss, and R. Morandotti, Cross-polarized photon-pair generation and bichromatically pumped optical parametric oscillation on a chip, Nat. Commun. **6**, 8236 (2015).

[25] I. S. Grudinin and N. Yu, Dispersion engineering of crystalline resonators via microstructuring, Optica **2**, 221 (2015).

[26] M. Förtsch, J. U. Fürst, C. Wittmann, D. Strekalov, A. Aiello, M. V. Chekhova, C. Silberhorn, G. Leuchs, and C. Marquardt, A versatile source of single photons for quantum information processing, Nat. Commun. **4**, 1818 (2013).

[27] Z. Y. Ou and Y. J. Lu, Cavity Enhanced Spontaneous Parametric Down-Conversion for the Prolongation of Correlation Time between Conjugate Photons, Phys. Rev. Lett. **83**, 2556 (1999).

[28] H. Wang, T. Horikiri, and T. Kobayashi, Polarization-entangled mode-locked photons from cavity-enhanced spontaneous parametric down-conversion, Phys. Rev. A **70**, 043804 (2004).

[29] F. Wolfgramm, Y. A. de Icaza Astiz, F. A. Beduini, A. Cere, and M. W. Mitchell, Atom-Resonant Heralded Single Photons by Interaction-Free Measurement, Phys. Rev. Lett. **106**, 053602 (2011).

[30] X.-H. Bao, Y. Qian, J. Yang, H. Zhang, Z.-B. Chen, T. Yang, and J.-W. Pan, Generation of Narrow-Band Polarization-Entangled Photon Pairs for Atomic Quantum Memories, Phys. Rev. Lett. **101**, 190501 (2008).

[31] D. Rieländer, A. Lenhard, O. J. Farìas, A. Máttar, D. Cavalcanti, M. Mazzera, A. Acín, and H. de Riedmatten, Frequency-bin entanglement of ultra-narrow band non-degenerate photon pairs, Quantum Sci. Technol. **3**, 014007 (2017).

[32] H. Zhang, X.-M. Jin, J. Yang, H.-N. Dai, S.-J. Yang, T.-M. Zhao, J. Rui, Y. He, X. Jiang, F. Yang, G.-S. Pan, Z.-S. Yuan, Y.-j. Deng, Z.-B. Chen, X.-H. Bao, S. Chen, B. Zhao, and J.-W. Pan, Preparation and storage of frequency-uncorrelated entangled photons from cavity-enhanced spontaneous parametric downconversion, Nat. Photonics **5**, 628 (2011).

[33] D. Rieländer, Kutlu Kutluer, PatrickM Ledingham, Mustafa Gündoğan, Julia Fekete, Margherita Mazzera, and Hugues de Riedmatten, Quantum Storage of Heralded Single Photons in a Praseodymium-Doped Crystal, Phys. Rev. Lett. **112**, 040504 (2014).

[34] F. Wolfgramm, C. Vitelli, F. A. Beduini, N. Godbout, and M. W. Mitchell, Entanglement-enhanced probing of a delicate material system, Nat. Photonics **7**, 28 (2013).

[35] T. Harty, D. Allcock, C. J. Ballance, L. Guidoni, H. Janacek, N. Linke, D. Stacey, and D. Lucas, High-Fidelity Preparation, Gates, Memory, and Readout of a Trapped-Ion Quantum Bit, Phys. Rev. Lett. **113**, 220501 (2014).

[36] J. W. Britton, B. C. Sawyer, A. C. Keith, C.-C. J. Wang, J. K. Freericks, H. Uys, M. J. Biercuk, and J. J. Bollinger, Engineered two-dimensional Ising interactions in a trapped-ion quantum simulator with hundreds of spins, Nature **484**, 489 (2012).

[37] Z.-Q. Zhou, W.-B. Lin, M. Yang, C.-F. Li, and G.-C. Guo, Realization of Reliable Solid-State Quantum Memory for Photonic Polarization Qubit, Phys. Rev. Lett. **108**, 190505 (2012).

[38] F. Torabi-Goudarzi and E. Riis, Efficient cw high-power frequency doubling in periodically poled KTP, Opt. Commun. **227**, 389 (2003).

[39] R. Rangarajan, M. Goggin, and P. Kwiat, Optimizing type-I polarization-entangled photons, Opt. Express **17**, 18920 (2009).

[40] M. Scholz, L. Koch, and O. Benson, Statistics of Narrow-Band Single Photons for Quantum Memories Generated by Ultrabright Cavity-Enhanced Parametric Down-Conversion, Phys. Rev. Lett. **102**, 063603 (2009).

[41] J. Yang, T.-M. Zhao, H. Zhang, T. Yang, X.-H. Bao, and J.-W. Pan, Realization of double resonance for a bright frequency-tunable source of narrowband entangled photons, Chin. Phys. B **20**, 024202 (2011).

[42] See Supplemental Material at http://link.aps.org/supplemental/10.1103/PhysRevApplied.10.054036 for details of the the SFG progress, cavity-SPDC process, and the methods to improve this source, which includes Refs. 40 and 41.

[43] E. D. Black, An introduction to Pound-Drever-Hall laser frequency stabilization, Am. J. Phys. **69**, 79 (2001).

[44] M. Schug, J. Huwer, C. Kurz, P. Müller, and J. Eschner, Heralded Photonic Interaction between Distant Single Ions, Phys. Rev. Lett. **110**, 213603 (2013).